Modeling correlation between radial distribution of pores volume and temperature in high burn-up UO_2 pellet

Suwardi
Center for Nuclear Technology – National Nuclear Energy Agency BATAN
PUSPIPTEK, Serpong, Banten-15310 Indonesia
**email: suwardi@batan.go.id*

Abstract
Temperature distribution has been evaluated by using different model of pore distribution. Pellet pore and its distribution change with burnup, especially in radial direction. Typical high burnup data of radial distribution of power density and porosity have been chosen in this study. Different pore distribution models have been studied for related temperature, in correlation with high burn up thermal properties. Both pore and temperature distributions have strong influence on thermal conductivity, then on temperature distribution. Finite element method has been developed for resolving the implicit temperature distribution from the governing non-linear system differential equations of heat transfer. The effect of number of elements on calculated temperature has been studied, and it shows exponential relation, which effect reduce to under 1 % when the number of radial elements > 25. Above the number, there is no significant different result. At high burnup, the pore is very high at rim zone and nearly homogenous at other radial position while the temperature distribution is nearly parabolic with radial position with peak at pellet center. The antagonist effect has been calculated as combined correction factor, which shows a maxima and minima value at radial position ~ 0.8 and ~ 0.9 respectively. The pore distribution at high burnup decreases the thermal conductivity ~ 10 % of outer radial zone of pellet. Because the outer surface of pellet temperature is fixed, the different pore models resulted in different of peak temperature at the center of pellet. Comparison of the temperature modeling distribution and the measured one permit the determination of best choice of pore model.

Keywords: UO_2 pellet, high burnup, pore, temperature, distribution.

Abstrak
Distribusi temperatur telah dievaluasi dengan menggunakan model yang berbeda dari distribusi pori. Pori pelet dan distribusi dengan derajat bakar berubah terutama dalam arah radial. Data derajat bakar tinggi khas distribusi radial dari kerapatan daya dan porositas telah dipilih dalam penelitian ini. Model distribusi pori yang berbeda telah dipelajari untuk suhu terkait dalam korelasinya dengan sifat termal pada derajat bakar tinggi. Kedua distribusi memiliki pengaruh yang kuat pada konduktivitas termal, selanjutnya pada distribusi temperatur. Metode elemen hingga telah dikembangkan untuk menyelesaikan distribusi temperatur implisit dari sistem persamaan diferensial non-linear dari perpindahan panas. Pengaruh jumlah elemen pada suhu dihitung telah dipelajari, dan itu menunjukkan hubungan eksponensial, efek itu menurun. hingga <1% bila jumlah elemen radial> 25. Di atas jumlah itu tidak menghasilkan beda signifikan. Pada derajat bakar tinggi pori-pori sangat tinggi di zona luar dan hampir homogen pada posisi radial lainnya, sedangkan distribusi temperatur hampir parabola dengan posisi radial dengan puncak pada pusat pelet. Efek antagonis telah dihitung sebagai gabungan faktor koreksi, yang menunjukkan maxima dan minima nilai pada posisi radial ~0,8 dan ~0,9 . Distribusi pori pada derajat bakar tinggi menurunkan konduktivitas termal dari 10% radial luar pelet. Karena permukaan luar suhu pelet adalah tetap, model pori yang berbeda menghasilkan beda suhu puncak di pusat pelet. Model yang baik dapat dipilih dengan

pembandingan distribusi temperature dari berbagai model faktor koreksi pori dengan data eksperimen.

Kata kunci: UO_2 pelet, derajat bakar tinggi, pori, suhu, distribusi.

1. Introduction

Up to date no NPP has been operated in Indonesia. It had been planned to be built a first NPP in 90 decade. The plan of NPP introduction has been revised to become 2005. The revision has been revised agains caused by the severe monetary and economic crisis in last years of last millennium. The last study concludes national energy policy for energy program that NPP must be introduced in 2016 to national energy system in 2016 [1]. KEN – vision 20/20, in 2020 the share of new and renewable energy of national nuclear energy should attain 20%. Nuclear energy should contribute ~ 2% of national electricity [1,2].

In the past, the burn-up of LWR fuel averaged about 33 MWD/kg. More efficient use of nuclear fuel has been continuously performed for cheaper nuclear electric since the movement of counter nuclear power trends increase. An increase to 100 MWD/kg is within technical reach, and even greater increases are potentially achievable. Increasing the burn-up to 100 MWD/kg would yield a three folds reduction in the volume of spent fuel to be stored, conditioned, packaged, transported, and disposed of per unit of electricity generated [3,4] The corresponding reduction in the required repository storage volume would be more modest; the individual fuel assemblies. A further benefit of higher burn-up is that the isotopic composition of the discharged plutonium would make it less suitable for use in nuclear explosives. By the way, there are more phenomena appear only after fuel pin has reached high burnup such HBS, steeper radial distribution profile of porosity. These phenomena need to be well understood to assure the understood to assure the safety and efficiency of fuel during irradiated in reactor core.

The properties of the High Burn-up Structure (HBS) at the pellet rim on thermal performance and fission gas release. A trend towards increasing the discharge burnup of nuclear fuel has been a feature of the operation of all types of nuclear power plant for many years. The increase of fuel burnup, and a concurrent increase in fuel duty, has been implemented in response to the economic challenge to reduce costs associated with nuclear power. Increased in-reactor life time allows smaller fuel inventories, and reduced spent fuel arising, but there are also increased costs associated with high burnup, for example, increased enrichment and meeting new challenges to fuel integrity and performance. Increased burn-up has been achieved through continuous development of fuel materials, especially advanced cladding, careful and incremental experimentation. Specific behaviour of high burnup oxide fuel is caused for the most part by [5]: 1) degradation of the lattice heat conductivity; 2) development of the gaseous porosity of different origin; 3) formation of radial profiles in distribution of plutonium and burnup, restructuring at the pellet periphery; 4) collapse of the gap, physic-chemical and mechanical pellet-cladding interaction; 5) degradation of the cladding mechanical properties. The existing of HBS has been confirmed at high burnup by many researchers after firstly reported by Ref. [6].

The nuclear fuel is one of the key elements which have to be acted upon if utilities are to be helped to fulfill their mission of generating power in total safety and supplying the kWh to their customers at the best price [6]. In order to determine the most economic level of discharge

burn-up in reactor nuclear fuel analysis is performed. With increasing burn-up of light water reactor (LWR) fuels, it becomes more important to estimate the irradiation behavior of the fuel pellets. In the thermal-mechanical analyses, the fuel temperature and its distribution in spatial and time are the prime parameters for calculation of other parameters. Thermal conductivity of fuel pellets is strongly depends on pore distribution. Initial pore distribution of fresh pellet that is fabrication pores is homogeneous and after irradiation fabrication pores may disappears by thermal but neutrons flux and energetic fissions fragment and farther irradiation resulting fission product solid and gas. Fission gas may precipitate to form gas bubbles pores which decreases significantly its thermal conduction. It is one of the most important thermal properties for calculating the fuel temperature during irradiation. The pores generation and distribution depend on differ parameters, then for a realistic prediction a comprehensive code is needed.

There are numerous effects of the over 100 different nuclides produced by fission of nuclear fuel. The elemental composition of fission products continuously changes with burnup by radioactive decay even as their concentrations increase. The chemical forms of individual fission product elements depend upon temperature and oxygen potential. The rare gases xenon and krypton are produced in one out of four fissions. These elements do not react chemically but exist as elements in the fuel either as single atoms in the crystal lattice or as inter-granular or intra-granular bubbles [7]. The partition of the fission gas between these two states determines the swelling of the fuel and gap pressure which both increase thermal conductance of gap.

For studying an individual phenomenon and in addition of lacking integral fuel code, an individual phenomenon modeling as pore distribution relation to thermal and temperature distribution is a good approach.

The paper presents a study about the effect of pore distribution at high burn-up on fuel temperature. The temperature distribution has been obtained by applying a simple model of steady-state heat transfer of fuel rod at particular level of high burnup. Calculation has been done by typical models of pore distribution and gap conductance at high burnup. The model takes into account thermal properties dependent of pellet to temperature, pore, and burnup.

1. Methodology

The thermal conductivity changes of irradiated UO_2 and (U, Gd)O_2 pellets may be related to different phenomena such irradiation-induced point defects, fission products and irradiation- induced micro bubbles. The degradation of thermal conductivity related to high burnup has long been studied, but still all be fully understood. The formation of HBS (rim structure at high burnup) that contains more pores has been studied for long time. In this study some models of relation between porosity and temperature to thermal conductivity of irradiated UO2 fuel has been chosen to calculate the temperature distribution in the fuel rod when pore distribution is given.

The temperature distribution has been obtained by applying a simple model of steady-state heat transfer of fuel rod at particular level of high burn-up. Calculation has been done by typical models of pore distribution and gap conductance at high burn-up. The model takes into account thermal properties dependent of pellet to temperature, pore, and burn-up. The procedure evolves the following steps.

Choosing the pore distribution data at high burn-up, model the temperature dependent of pellet conductivity, and temperature on cladding thermal conductivity. Pore contribution is modeled as factor to pellet thermal conductivity,

computes coolant water temperature along rod side related to the model of axial power distribution that is considered as cosines type. The cladding surface to water coolant heat transfer is calculated according to simplified model of Dittus-Boelter as the default option in Transuranus [8]. The temperature of cladding surface is chosen without taken into account thermal conductivity of CRUD. The gap conductance is calculated as given parameter. The radial power distribution is modeled as a linear combination function, fitted from typical density from experimental data. Rod heat transfer in the axial direction is omitted. Heat transfer equation in the fuel pellet is approached by a combination of finite element and finite differences Saturn-FS1[9].

2.1. Pore distribution.

Pore distribution is obtained by linear combination fitting an experimental data [9], and modification for this parametric study.

$$por(y) := \begin{cases} 0.05\cdot\frac{Power(y)}{0.375} & \text{if } y < 0.8 \\ 0.05\cdot\frac{Power(y)}{0.375} + (y-.8)\cdot 1.6 & \text{if } 0.8 \le y \le 0.9 \\ 0.05\cdot\frac{Power(.9)}{0.375} + 0.16 & \text{if } 0.9 < y \end{cases} \quad (1)$$

A modified expression for this study for example :

$$pori(y) := \begin{cases} 0.05\cdot\frac{Power(y)}{0.375} & \text{if } y < 0.8 \\ 0.05\cdot\frac{Power(y)}{0.375} + (y-.8)\,1.6 & \text{if } (0.8 \le y < 0.85) \\ 0.05\cdot\frac{Power(y)}{0.375} + (y-.8)\,2.0 & \text{if } 0.85 \le y < 0.91 \\ 0.05\cdot\frac{Power(.9)}{0.375} + 0.16 & \text{if } 0.94 < y \end{cases} \quad (2)$$

2.2. Pore and thermal conductivity.

Two models of thermal conductivity of irradiated fuel is applied:

a. Correction factor for fuel pore that is modeled as pure pore variable of

$$Fp : \frac{1.1316\cdot(1-por)}{1+\left(por+10\cdot por^2\right)} \quad (3)$$

b. Correction factor of pore that depends on pore and a coefficient depending temperature. The measured thermal conductivities were normalized to the values of 96.5%TD (TD: theoretical density) by using the Loeb's equation:

$$^{a}n = {}^{a}m(1-0.035\,£)\,/\,(J-£P), \quad (4)$$

Where: ^{a}n is the thermal conductivity normailized to that of 96.5% TD; ^{a}m the measured conductivity, £ the parameter which express the effect of pore shape on the thermal conductivity of pellets, and P the porosity evaluated from the sample density. The parameter £ is expressed as follows [10]:

$$£ = 2.6\text{-}5\times10^{-4}(T(K)-273.15), \quad (5)$$

F, pore factor given by

$$F = 1.0 - 2.5\cdot P \quad (6)$$

Where $P = 1 - TD$

The last two models may be unified as correction factor of wiesenak.

$$Fp = (1- \quad .P)\,/\,(1\text{-}0.05^{*} \quad) \quad (7)$$

Where

$$= 2.58 - 0.58\text{x}10^{3}.T, \quad T=Tc$$

$$K = K_{95\%TD}\cdot(1- \quad p)\,/(1-0.05\ (W/mK) \quad (8)$$

MatPro V 9.0 model of temperature dependent of thermal conductivity of fresh / un- irradiated UO_2 Fuel has been chosen.

For: $0 < T < 1650^{o}C$

$$K\_mp\_(\beta,D,T) := \left(\frac{-\beta(1-D)}{1-0.05\beta}\right)\cdot\left(\frac{40.4}{.464+T}+1.216\times10^{-4}\cdot\exp(1.867\times10^{-3}T)\right) \quad (9)$$

and for: 1659 < T < 2840°C

$$K\_sup\_b(5,D,T) := \left[\frac{1-\beta(5,D)}{1-0.65}\right]\cdot\left[3.09+2.26\cdot10^{-4}\cdot\exp(1.567\cdot10^{-3}\cdot T)\right] \quad (10)$$

The computation and results visualization are performed within MathCAD environment. The equations presented here are MathCAD format, and there is a slight difference with conventionally mathematical expression

2.3 Coolant temperature along the channel

The surface temperature *Ts* at each axial location of the fuel rod is the starting point for calculation of the radial temperature distribution of related *z* position. The flowing coolant temperature is calculated from the energy balance of fuel and coolant system, local and total along the fuel rod.

$$T_{cool}(z) := \begin{cases} T_{in} + \dfrac{1}{Qm_W \cdot cp_W}\cdot\int_0^z qr(z)\,dz & \text{if } ty = 1 \\ T_{sat} & \text{if } ty = 2 \end{cases} \quad (11)$$

Qm_W is mass flow rate of coolant, cp_W is the heat capacity of the coolant - temperature dependent, T_{cool} is coolant temperature and T_{in} is inlet coolant temperature. The parameter to represent reactor type 1 for LWR and 2 for PWR. The linear power, *qr(z)*, is position dependent as follow [10]:

$$qr(z) := \cos\left[\pi\left(\frac{z}{3.L}-0.25\right)\right]-\sin\left[\pi\left(\frac{z}{3.L}-0.3\right)\right]-1.q0 \quad (12)$$

Where *q0* is Linear Heat Generation Rate and *L* is fuel rod length.

2.4 Cladding Surface Temperature

In the analysis a single-phase heat transfer model simplifies the heat transfer coefficient of cladding surface. The Dittus-Boelter equation for heat transfer coefficient has been chosen:

$$hw = 0.023\cdot\left(\frac{k}{De}\right)\cdot\left(\frac{De\cdot v\cdot\rho}{\mu}\right)^{0.2}\cdot Pr^{0.4} \quad (13)$$

is reduced by choosing the right hand side with the mean value, except the coolant thermal conductivity. The surface temperature of cladding in *z* position (*Tcl(z)*) is then calculated, knowing the linear power *qr(z)* and the convective heat transfer coefficient *(hw)*.

$$Tcl(z) := Tcool(z) + \frac{qR(z)}{2\pi\cdot hw} \quad (14)$$

2.5. Radial Distribution of Cladding Temperature

Discretion of cladding, using the term of cladding radius *(rc)*, *nc* = number of cladding segment, *Rci* inner cladding radius and *Rco* for outer cladding radius. The range of cladding radius *rc* is:

$$rc := \left(Rci, Rci + \frac{Rco-Rci}{nc-1} \cdots Rco\right) \quad (15)$$

The cladding temperature is calculated from the energy balance around the cladding. The balance around a slice of cladding ring, omitting the cladding water side corrosion, can be arranged as:

$$Tc(rc) := T_{clo} + \frac{qz_0}{2\pi\cdot\lambda cl(Tc)}\ln\left(\frac{Rco}{Rc}\right) \quad (16)$$

Tc(rc) is temperature of cladding at *rc*. *Tc(Rco)* is the temperature of outer cladding. λcl is thermal conductivity of cladding. Iteration is needed since the equation contains an implicit variable.

The difference between inner and outer cladding surfaces is:

$$Tc(Rci) - Tc(Rco) - \frac{qz_0}{2\pi\lambda cl(Tc)} \ln\left(\frac{Rco}{Rci}\right) \quad (17)$$

At this point the temperature of flowing coolant to the inner surface of cladding is known. The outer surface of fuel pellet than is calculated using a simplified input of gap conductance. It is assumed that the gap distance is not change by difference temperature distribution caused be non-heterogeneity of power:

$$\Delta T_{gap} = \frac{qz_0}{2\pi . Rf . \lambda_{gap}(T)} \quad (18)$$

2.6 Radial Distribution of Fuel Temp and Porosity

The heat transfer from pellet surface to the inner surface of cladding is calculated using a simplified correlation of gap conductance as a temperature function.

The radial heat transfer in the solid pin is much higher than in axial direction then axial heat transfer is neglected. The energy balance in the fuel contains a power density term depends on the corresponding radius,

$$-\lambda(T(r), por(r))\frac{dT(r)}{dr} = \frac{1}{2\pi} qr(r) \quad (19)$$

The *qv(r)* is volumetric power density profile according to radial coordinate, be modeled as polynomial Eq.(10) that is fit of typical power distribution.

$$qv(r) = p \; . \; v(r) \quad (20)$$

For high burn-up the polynomial is expressed by Eq. (21):

$$p = \begin{pmatrix} 0.373 \\ 0.22 \\ 0.410 \end{pmatrix} \quad \text{and} \quad v(x) = \begin{pmatrix} 1 \\ x^{12} \\ x^{24} \end{pmatrix} \quad (21)$$

The correlation between linear power density/LHGR *qr(r)* and volumetric power density *qv(r)* is:

$$qr(r) = 2.\pi.\int nt\{.r.qv(r).dr\} \quad (22)$$

A finite element approach is applied for the radial distribution of fuel temperature. The radial space is discretized into nr element of linear Lagrangian type. Fuel temperature in each element is defined as:

$$T(r) - \frac{T_k.(r_{k+1} - r) + T_{k+1}.(r - r_k)}{r_{k+1} - r_k} \quad if \; r_k \le r \le r_{k+1} \quad (23)$$

T_k, and T_{k+1}, is temperature at corresponding nodal coordinate (K_r, r_{k+1}) with global numbering.

The *qr* is power (thermal) generated by cylindrical fuel with radius = *r* per unit length. qr is given as a polynomial of *r* variable obtained from fitting the curve of SATURN-FS1 figure.

If *p* represents volumetric density of power at radius *r*, with Eq.(14):

$$qr(r) = \frac{p_{k-1}.(r_{k+1} - r) + p_k.(r - r_k)}{r_{k+1} - r_k} \quad (24)$$

Qv (=average power generated per unit volume) can be calculated with equation 15. Here *q0* is *qr* at pellet surface, that is LHG (Linear Heat Generation)

$$Qv - \frac{q0}{0.25.\pi.Dp^2} \quad (25)$$

Introducing three new variables *Ai*, *Bi*, and *R* as follow:

$$R - \frac{(rf_{nR})^2 \quad (rf_0)^2}{\sum_{i}^{nR}(A_i.pm + B_i.pp)} \quad (26)$$

$$A_i - \begin{cases} 10^{-7} & if \; i - 0 \\ \frac{1}{3}(r_i - r_{i-1})(r_{i-1} + 2r_i) & if \; i \neq 0 \end{cases} \quad (27)$$

$$B_i = \begin{cases} 10^{-6} & if\ i = nR \\ \frac{1}{3}(r_{i+1} - r_i)(2r_i + r_{i+1}) & if\ i \neq nR \end{cases} \quad (28)$$

Then, the volumetric power generation can be written as:

$$qr_k = ®.R.Q_v(B_k.p_k + A_{k+1}.p_k) \quad (29)$$

By using finite different approach, the energy balance Eq. (13) becomes:

$$-\lambda(T(r), por(r))\frac{T_{k+1} - T_k(r)}{r_{k+1} - r_k} = \frac{1}{\pi(r_{k-1} + r_k)} qr\left(\frac{1}{2}(r_k - r_{k-1})\right) \quad (30)$$

T_k is fuel temperature at node *k*. It can be written explicitly.

$$T_k = T_{k-1} + D_k \frac{qr\left(\frac{1}{2}(r_k + r_{k-1})\right)}{\lambda(T(r), por(r))} \quad (31)$$

$$D_i = \begin{cases} 10^{-2} & if\ i = nR \\ \frac{(rf_{i+1} - rf_i)}{(rf_{i+1} + rf_i)} & if\ i \neq nR \end{cases} \quad (32)$$

Substitution of *qr* in Eq. (19) into Eq. (21) and using variables *Qv* in Eq. (15), while *A* Eq. (16), *B* Eq. (22) and new variables *F, G, AA, BB* as Eq. (23) to next Eq. (26):

$$F_i = \begin{cases} 10^{-8} & if\ i = nR \\ \frac{1}{12}\frac{7rf_i + 2rf_{i+1}}{rf_{i+1} + rf_i}(rf_{i+1} - rf_i)^2 & if\ i \neq nR \end{cases} \quad (33)$$

$$G_i = \begin{cases} 10^{-8} & if\ i = nR \\ \frac{1}{12}\frac{2rf_i + 2rf_{i+1}}{rf_{i+1} + rf_i}(rf_{i+1} - rf_i)^2 & if\ i \neq nR \end{cases} \quad (34)$$

$$AA_i = \sum_{j=1}^{nR-i} \left(A_j.pp + B_j.pm\right) \quad (35)$$

$$BBi = FnR\text{-}i\ .\ pp + GnR\text{-}i\ .\ pm \quad (36)$$

Eq. (21) can be rewritten:

$$T_j = T_{j-1} + D_i \frac{Qv}{\lambda(T(r), por(r))}\left[Qv.R.D_{nR-i}.\left(AA_i + A_{nR-i}.pm\right) + BB_i\right] \quad (37)$$

The two constants p_p and p_m in *AA* and *BB* are correction factors. For this analysis they are sufficiently set as 1.0. Now the radial temperature distribution of z position is established. For other z coordinate the different in q_r and *Tcool*. *Tcool(z)* has been calculated in eq-1. Linear heat generation (*qr* at radial position *R*) for different *Z* is LHGR multiplied by the axial power-factor. Repeating the radial distribution for all axial position using corresponding coolant temperature in eq-1, and volumetric heat generation Eq. (10) the temperature distribution in 2-dimensional space is calculated. Comparing the temperature distribution does the analysis and the corresponding thermal property calculated by different heterogeneity of power density in radial or in axial direction.

Result and Discussion

Fig.1 shows the temperature obtained by different number of radial discretion of pellet. About 25 or more radial-elements are needed for accurate numerical results. Fig. 2 shows the axial temperature distribution of outer surface cladding and coolant temperature. The profile of pin temperature is nearly cosine type caused by axial profile of LHGR. The coolant temperature rises axially from thermal power along the fuel pin.

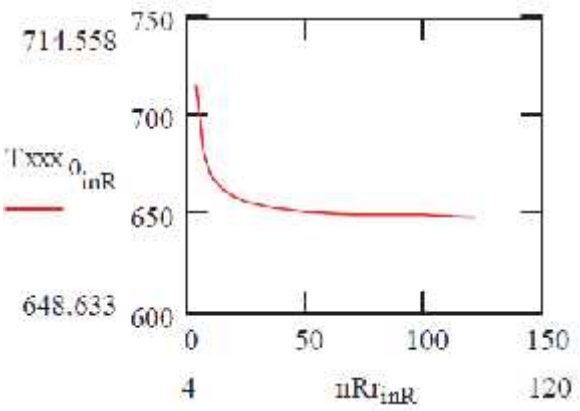

Fig.1. Effect of fine discretization on numerical Results.

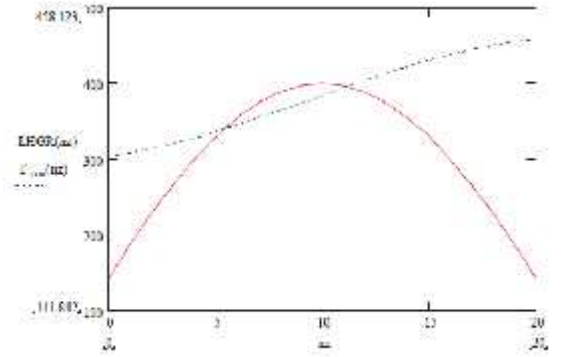

Fig.2. Axial temperature distribution of outer surface cladding and coolant temperature.

Explain below about figure (graphic): Fig. 3 shows the model of pore effect on thermal conductivity according to Eq. (7), and Eq. (4) and Eq. (5). Fig. 4 shows the model of temperature effect on thermal conductivity, is part two of Eq. (9). Fig. 5 shows the two models of radial pore distributions eq-2 and Eq-2. Fig. 6 shows the effect of radial temperature distribution on thermal conductivity. As expressed by second parenthesis of Eq. (9). Fig. 7 represents effect of radial pore distribution on thermal conductivity of the 2 pore distributions. Fig. 9 shows combination effect of temperature and pore distribution on pellet thermal conductivity related to Fig. 7. The effect rise gradually according to radial position until it approaches the HBS that suddenly falls to the minimum value, and then rise again as temperature decrease in radial direction. Fig.8 shows 3 profiles of pore correction factor of thermal conductivity along pellet radius resulted from two pore distributions.

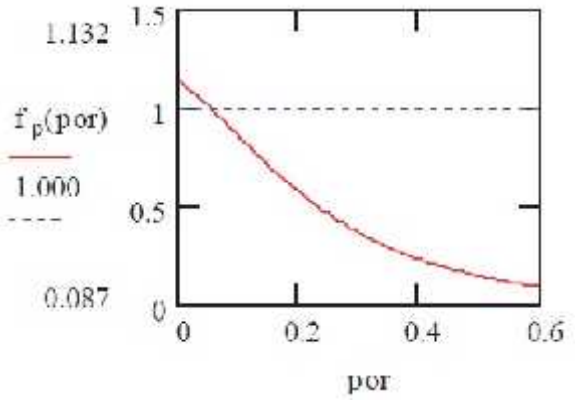

Fig.3. Model of pore effect on thermal conductivity.

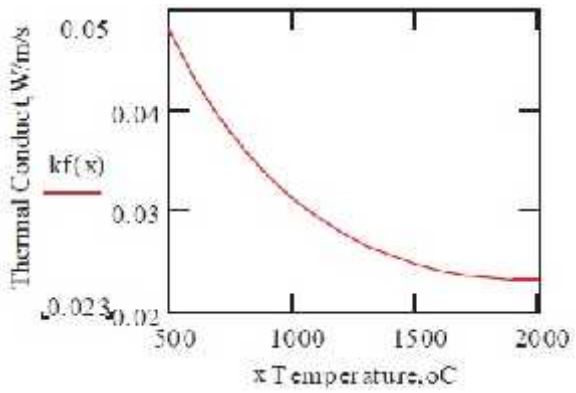

Fig. 4. Model of temperature effect on thermal conductivity.

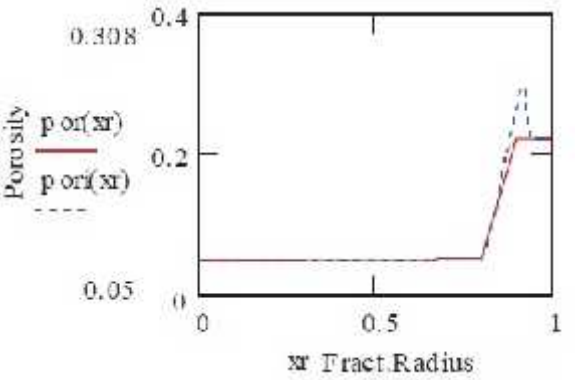

Fig. 5. Two models of radial pore distribution.

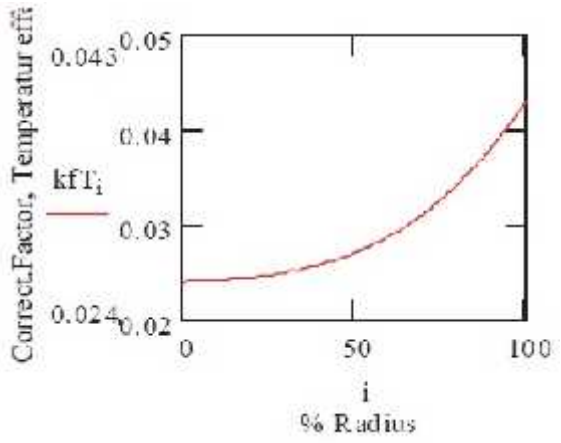

Fig.6. Effect of radial temperature distribution on thermal conductivity.

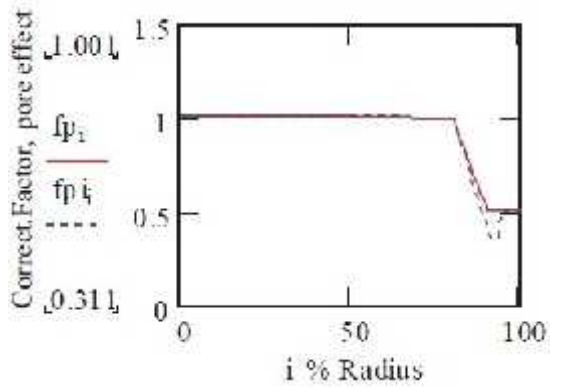

Fig.7. Effect of radial pore distribution on thermal conductivity.

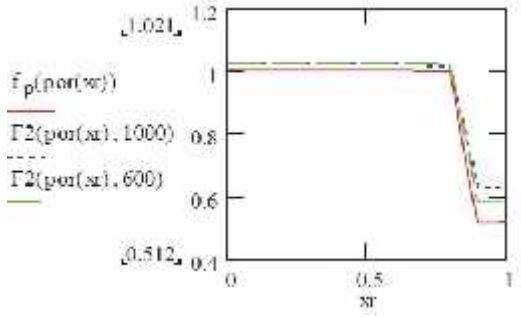

Fig. 8. Pore correction factor of thermal conductivity along pellet radius.

From three different pore distributions and two different pore correction factors resulted six different profile pore correction factors. An average of fist profile of correction factor has also been used to be calculated the temperature distribution in radial direction. The result is plotted in. Fig.11. The plot shows radial distribution of pellet temperature of different pore distribution. *Tp* is calculated by radial average of pore correction factor *Tp1* and *Tp11* use different model of core correction factor, *Tpfp, Tpf2*, different models of pore correction factor *Tp31, Tp3.*

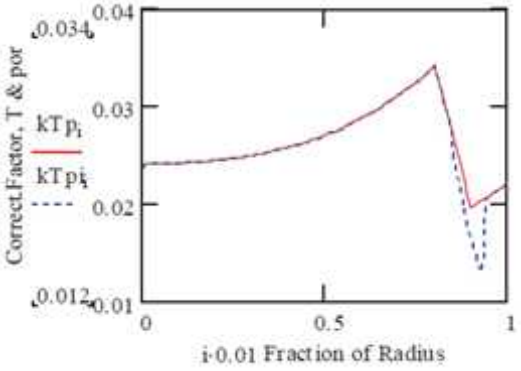

Fig.9. Two radial distribution of thermal conductivity by combination of local temperature and porosity (*kTp* by average and *kTpi* by local).

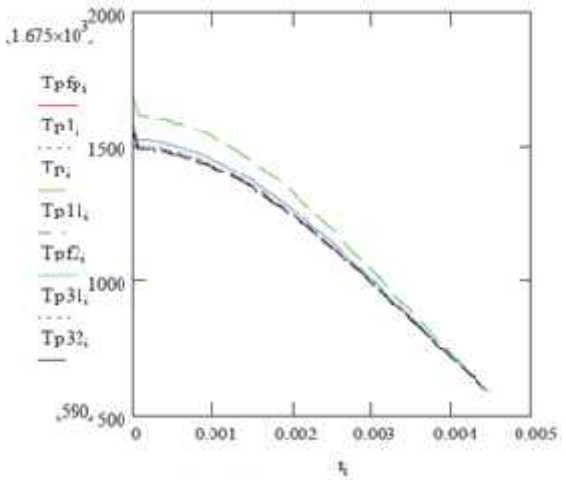

Fig. 10. Radial pellet temperature distribution of different pore distribution. Tp is calculated by radial average of pore correction factor.

Fig.11 shows a zoom of right part of Fig.10. Fig 12 shows zoom of left part of Fig 11. The temperature profile calculated by using average correction factor give a maximum deviation from the average, that is can be anticipated of not using the local correction factor. The plot results from two different models of correction factors are hardly differentiable. The two models give the same numerical results. A little different of pore distribution results a clear different temperature distribution (*Tpf* to *Tp*).

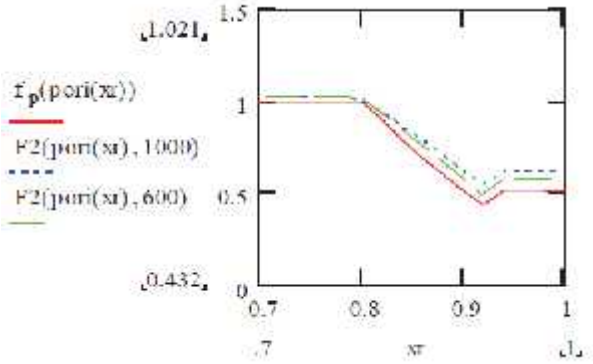

Fig. 11. Zoom of right part of Fig. 9.

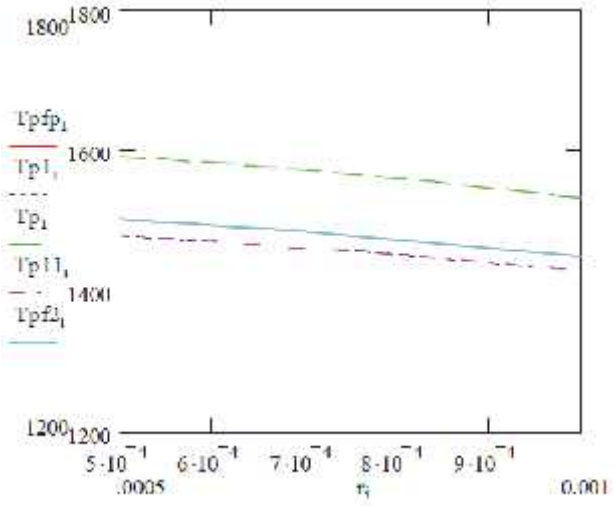

Fig. 12. Zoom of left part of Fig 10.

Temperature decrease radially. Fig.9 shows 3 profiles of pore correction factor of thermal conductivity along pellet radius resulted from two pore distributions.

4.Conclusion

A simple, steady state bi-dimensional axial symmetry model with a combination finite element - finite different approach has been used to study the relation between models of pore contribution to temperature distribution especially to centerline temperature. The model takes into account porosity and temperature for thermal conductivity and power density profile which resulting an implicit non-linear differential equation.

Calculation using mean correction factor, not local correction factor along diameter: resulting over-estimation 90 K of central line temperature.

The two models correlation of correction factor as function of pore and temperature resulting no significant different on resulted temperature.

Pore distribution need to be expressed well especially related to HBS to give accurate results of the central line temperature of pellet.

Acknowledgements

The author would like to thank Mr. Basak, Nuclear Fuel Cycle and Waste Technology Division, Nuclear Fuel Cycle and Materials Section - IAEA, for granting financial support for participation in IAEA CRP T12027.

References

[1] Anonym, Rencana Umum Energi Nasional, Proceeding The CASINDO Meeting, Grand Candi Hotel Semarang, 13 Juli 2011

[2] M. Girianna, Keselarasan Kebijakan Energi Nasional (KEN) dengan Rencana Umum Energi Nasional (RUEN) dan Rencana Umum Energi Daerah (RUED), Direktur Sumber Daya Mineral, Energi dan Pertambangan, Jakarta, 2012.

[3] J. Zhang, H. Druenne, Perspective on a Limited Burnup Extension for Belgian PWRs, High Burnup Fuel Experience and Economics, IAEA Technical Meeting, Sofia, Bulgaria, 2006, pp: 66-78

[4] D.O. Brasnarof, A.C. Marino, J.E. Bergallo and L.E. Juanicó, A New Fuel Design for Two Different HW Type Reactors, J. Sci. Tech. Nucl. Install., 2011(2011)15.

[5] T. Tverberg, W. Wiesenack, Fission gas release and temperature data from instrumented high burnup LWR

fuel, Technical and economic limits to fuel burnup extension Proceedings of a Technical Committee meeting held in San Carlos de Bariloche, Argentina, 15–19 November 1999, pp. 7-16.

[6] K. Nogita, K. Une, Nuclear Instruments and Methods in Physics Research Section B: Beam Interactions with Materials and Atoms, Volume 91, Issues 1–4, 1 June 1994, Pages 301–306.

[7] Hj. Matzke and M. Kinoshita, J. Nucl. Mater., 247(1997)108–115.

[8] K. Lassmann, C.T. Walker, J. van de Laar, F. Lindström, J. Nucl. Mater., 226(1995)1-8.

[9] H.J. Ritzhaupt et al., SATURN-FS 1, A computer code for thermo-mechanical fuel rod analysis, Kernforschungszentrum Karlsruhe, (1993), pp: 5-16.

[10] W.W. El-Wakil, Nuclear heat transport, International Textbooks Co., Lavoisier Publishing Coy. (1985), pp: 9-21.